J Mater Sci: Mater Electron (2015) 26:8484–8488
DOI 10.1007/s10854-015-3519-9

Fabrication and comparison of the photocatalytic activity of ZnSe microflowers and nanosheets

Xiuyan Li[1] · Bing Wei[1] · Jian Wang[3] · Xuefei Li[1] · Hongju Zhai[2] · Dandan Wang[3] · Yanqing Liu[1] · Yingrui Sui[1] · Qi Zhang[1] · Jinghai Yang[1]

Received: 7 April 2015 / Accepted: 20 July 2015 / Published online: 30 July 2015

Abstract ZnSe mciroflowers and nanosheets were successfully fabricated by annealing the corresponding precursor $ZnSe(en)_{0.5}$ hybrid (en = ethylenediamine), which were synthesized via a solvothermal process in ethylenediamine-water system without any surfactants. All the samples were characterized by XRD, SEM and TEM. The results show that the precursor $ZnSe(en)_{0.5}$ was converted into pure ZnSe by annealing with original morphology preserved. ZnSe microflowers were assembled from lots of rectangle nanosheets. Nanosheets and the nanosheets of microflowers have the same growth pattern. The photoluminescence and photocatalytic activity of ZnSe microflowers and nanosheets were investigated. The result shows that ZnSe microflowers exhibited superior photocatalytic activity and the reason was analyzed.

✉ Xiuyan Li
lixiuyan@126.com

✉ Jinghai Yang
jhyang1@jlnu.edu.cn

[1] Key Laboratory of Functional Materials Physics and Chemistry of the Ministry of Education, Jilin Normal University, Siping 136000, Jilin, People's Republic of China

[2] Key Laboratory of Preparation and Applications of Environmental Friendly Materials of the Ministry of Education, Jilin Normal University, Siping 136000, Jilin Province, People's Republic of China

[3] Changchun Institute of Optics, Fine Mechanics and Physics, Chinese Academy of Sciences, Changchun 130033, People's Republic of China

1 Introduction

In the past decades, semiconductor photocatalysts have attracted considerable attention in the fields of catalysis and photochemistry due to their high photocatalytic activity and broad applications in solving environmental pollutants in aqueous phase as well as in gaseous media [1, 2]. Among various semiconductor photocatalysts, ZnSe is considered as an effective catalyst for photocatalytic degradation of organic pollutants because of its wide direct band gap (2.67 eV) at room temperature and large exciton binding energy (21 meV) [3–5]. Recently, the photocatalytic activity of ZnSe micro/nanostructures has received much attention [6–9]. Qian et al. [6] reported that the photocatalytic ability of ZnSe nanobelts is stronger than that of the TiO_2 nanoparticles in the photodegradation of fuchsin acid solution under UV light irradiation.

It is generally accepted that the smaller size of micro/nanomaterials will exhibit superior photocatalytic activity. This is because smaller size of the micro/nanomaterials has high specific surface area. As we know, the photocatalytic process depends strongly on the adsorption and desorption of molecules on the surface of the photocatalyst. The large specific surface area can provide more reactive adsorption/desorption sites for photocatalytic reactions. However, photocatalysis reaction is a complicated process and the photocatalytic activity of micro/nanomaterials was influenced by many factors rather than sample size. Yang et al. [10] reported that ZnSe nanosheets with a length of up to 4 μm exhibited superior photocatalytic activity compared to the ZnSe nanoparticles (average size of approximately 7 nm) because ZnSe nanosheets have more surface defects exist in the nanosheets. Therefore, it is difficult to judge the photocatalytic activity of micro/nanomaterials only from the size of micro/nanomaterials.

In recent years, various morphologies and sizes ZnSe micro/nanostructures have been fabricated by a variety of methods, including quantum dots [11–14], nanoparticles [15], nanowires [16–19], nanosheets [20, 21], microrods [22], nanobelts [23, 24], nanospirals [25] nanotubes arrays [5, 26], and microflowers [4, 9, 27, 28]. However, these works were mainly focused on fabricating different dimensionality and size products rather than the photocatalytic properties of ZnSe micro/nanostructures. Furthermore, understanding of the relationship between microstructure and the photocatalytic properties of ZnSe is also significant. Therefore, fabricating a new type ZnSe architecture by a simply and low-cost synthetic strategy and investigating its photocatalytic properties still remains a great challenge in the area of materials research.

Among various synthesis methods, solvothermal method has attracted a lot of interest because it is simple and environmentally friendly. Generally, the precursor $ZnSe(en)_{0.5}$ was prepared by solvothermal method, and the ZnSe was obtained by annealing $ZnSe(en)_{0.5}$. The coordination of Zn^{2+} in $ZnSe(en)_{0.5}$ is similar to the $ZnSe_4$ tetrahedra in hexagonal ZnSe. $ZnSe(en)_{0.5}$ has a three-dimensional network. The two adjacent monlayers ZnSe layers are interconnected to each other by the nitrogen atoms in ethylenediamine molecules alone the a-axis [29]. In this paper, ZnSe microflowers and nanoosheets were synthesized by annealing the corresponding precursor $ZnSe(en)_{0.5}$ hybrid, which were synthesized via a solvothermal process in ethylenediamine-water system. All the samples were characterized by XRD, SEM and TEM. The optical properties and photocatalytic activities of ZnSe microflowers and nanosheets were also investigated.

2 Experimental section

2.1 Preparation

All reagents were purchased from Sinopharm Chemical Regent Co., Ltd, and used without further purification. The precursors $ZnSe(en)_{0.5}$ were synthesized by solvothermal method. In a typical procedure, appropriated amounts of $Zn(NO_3)_2{\cdot}6H_2O$ and Se powder (stoichiometry molar ratio 1:1) were dissolved in 60 mL ethylenediamine-deionized water solution (volume ratio 2:1). Namely, both $Zn(NO_3)_2{\cdot}6H_2O$ and Se powder have the same molar concentration. After stirring for 20 min at room temperature, the mixed solution was then transferred into a 100 mL Teflon-lined autoclave. The autoclave was sealed and maintained at 180 °C for 12 h, and then allowed to cool to room temperature naturally. After that, the precipitate (precursor) was washed with distilled water and ethanol for several times, dried overnight in a vacuum oven at 60 °C. To obtain ZnSe crystal, the as-prepared precursor was annealed under Ar atmosphere at 300 °C for 2 h.

2.2 Characterization

The crystalline structure of samples was determined using X-ray diffraction (XRD MAC Science, MXP18, Japan). The morphology and size of the as-synthesized samples were characterized by field emission scanning electron microscopy (FESEM, JEOL JEM-2010HR) and transition electron microscope (TEM, JEOL JEM-2010HR). The photoluminescence (PL) spectrum was preformed by a He–Cd Laser with a wavelength of 325 nm as the excitation source.

2.3 Photocatalysis

The photocatalytic activities of the as-prepared ZnSe samples were evaluated by degradation of RhB aqueous solutions (7 mg/L) under ultraviolet irradiation. The irradiation was afforded by a high-pressure Hg light, and the light wavelength was 365 nm. All experiments were carried out at room temperature. Before and after different irradiation intervals, the solution concentration of RhB was analyzed by a UV–Vis spectrophotometer (UV-5800PC, Shanghai Metash Instruments Co., Ltd).

3 Results and discussion

3.1 Characterization

Figure 1 shows the XRD patterns of these precursors prepared by different reactant concentration. The positions of the diffraction peaks are consistent with the values of $ZnSe(en)_{0.5}$ reported by Li et al. [30] and Lu et al. [31]. Notably, the precursor is $ZnSe(en)_{0.5}$. The strong and sharp

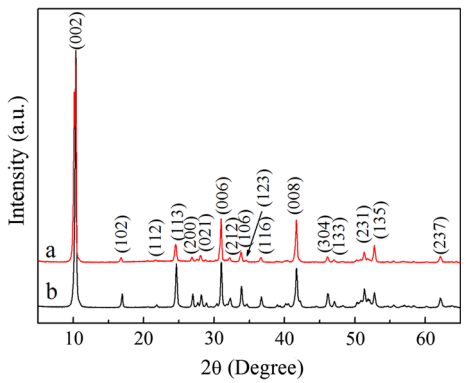

Fig. 1 XRD patterns of precursors prepared by different reactant concentration: *a* 0.008 mol/L, *b* 0.033 mol/L

diffraction peaks appearing in the XRD patterns indicate that the precursors have the well-crystallized.

The typical morphologyies of the as-synthesized precursor and ZnSe are shown in Fig. 2. When the reactant concentration is 0.008 mol/L, the as-synthesized precursor has flower-like structure, as shown in Fig. 2a. Acorroding to Fig. 2a, the flower-like structure is assembled from lots of rectangle nanosheets. The width and length of the nanosheet is respectively around 2 and 4 μm, and the thickness is quite thin, ca. 20 nm. Figure 2b shows that rectangle sheet-like precursor was synthesized when the reactant concentration is 0.033 mol/L. However, the sizes of these sheets are not homogeneous. The width of the sheets varies from 1 to 3 μm, and the length varies from approximately 2–6 μm. ZnSe crystal was obtained by annealing the precursors, and the SEM images are shown in Fig. 2c, d. No significant change in morphology has been observed after 2 h of thermal treatment at 300 °C. SEM image in Fig. 2c shows that the morphology of ZnSe is also microflowers, similar to that of the precursor, and the size of ZnSe were smaller than that of the precursor, which should be attributed to the loss of en in the precursor molecule. Likely, SEM analysis of Fig. 2d shows that annealing processes almost do not affect the morphology and size of nanosheets.

Figure 3 shows the XRD pattern of the as-synthesized ZnSe. When the $ZnSe(en)_{0.5}$ hybrid was thermally treated, its crystal structure changed completely. After 2 h of thermal annealing under Ar atmosphere, all the diffraction

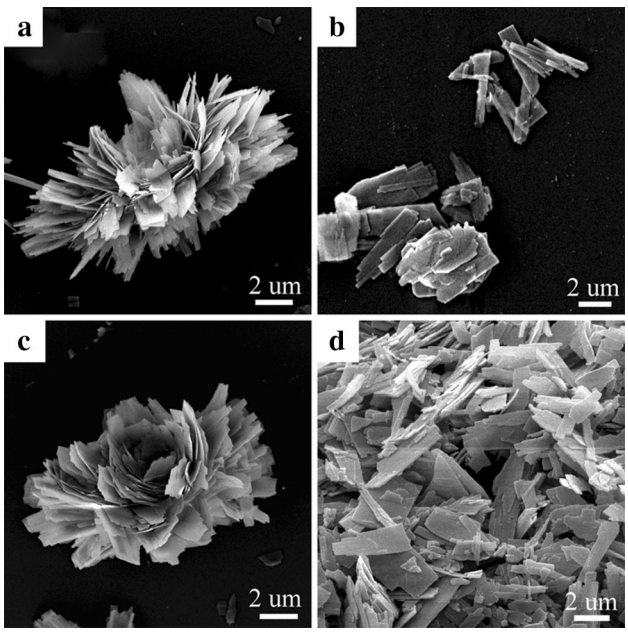

Fig. 2 SEM images of precursors and ZnSe prepared by different reactant concentration: **a**, **c** 0.008 mol/L, **b**, **d** 0.033 mol/L, respectively

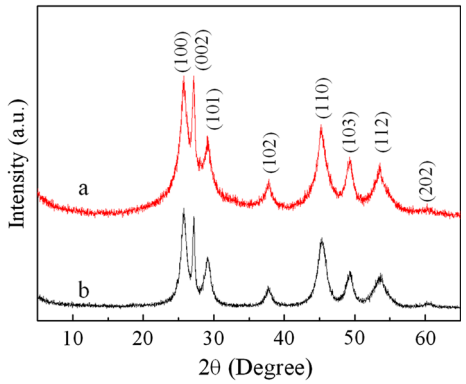

Fig. 3 XRD patterns of ZnSe after annealing the precursors prepared by different reactant concentration: *a* 0.008 mol/L, *b* 0.033 mol/L

peaks fit quite well the standard hexagonal wurtzite phase of ZnSe (JCPDS cards No. 80-0008). No other crystalline impurities were detected by XRD, indicating that pure wurtzite ZnSe can be obtained via this method.

The precursor $ZnSe(en)_{0.5}$ hybrid was yielded via a solvothermal reaction in ethylenediamine-water system. In precursor $ZnSe(en)_{0.5}$ structure, two adjacent monolayers ZnSe layers are connected to each other through the bonding of the nitrogen atoms in ethylenediamine molecules [30–32]. They form a three-dimensional network structure. When the $ZnSe(en)_{0.5}$ was annealed at 300 °C, it would be decomposed into ZnSe crystal accompanied by the chemical bonds rupture and removal of en molecules. The process of solid transformation from $ZnSe(en)_{0.5}$ to ZnSe is a topotatic transformation [33, 34], and the original morphology of precursor was preserved throughout the process. And in this process, ethylenediamine was used as a liquid medium and a structure-directing, coordinating molecular template that produce a particular morphology of sample. In addition, the results also indicate that the reactant concentration plays an important role in the morphology of the products.

To analyze the microstructure of ZnSe, further characterization by using TEM was carried out and the results were shown in Fig. 4. Figure 4a shows the TEM image of a single ZnSe microflower. The microflower is composed of numerous nanosheets with length about 4 μm, which is in good agreement with SEM observation in Fig. 3c. Figure 4b is HRTEM image from the solidlined rectangle in Fig. 4a. HRTEM image in Fig. 4b shows that the lattice spacing of 0.325 nm agrees well with the interplanar spacing of the (002) crystal planes of hexagonal wurtzite ZnSe, indicating that ZnSe sheet grows along [001] direction. At the same time, the HRTEM image in Fig. 4b further reveals that single crystalline structure of the each nanosheet of ZnSe microflower. Figure 4c and d show the TEM and HRTEM images of ZnSe nanosheets,

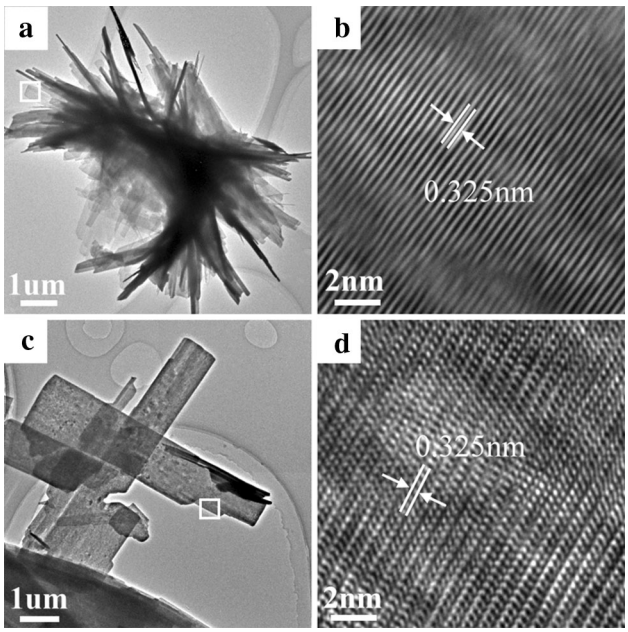

Fig. 4 TEM and HRTEM images of ZnSe microflowers (**a**, **b**) and nanosheets (**c**, **d**)

respectively. The TEM image reveals that ZnSe nanosheets are around 6 μm in length and 1 μm in width, which is in good coincident with the SEM observation. The fringe with lattice spacing (in Fig. 4d) of 0.325 nm matches well with the lattice spacing of the (002) plane of hexagonal wurtzite ZnSe. Clearly, ZnSe nanosheets grow also along the [001] direction and also exhibited a single crystalline nature. Based on the above analyses, a conclusion can be dawn that nanosheets and the nanosheets of microflowers have the same growth pattern.

3.2 Photoluminescence and photocatalysis

The room-temperature photoluminescence (PL) analysis of ZnSe samples were showed in Fig. 5. All PL spectra comprise of two emission bands: a strong emission peak centered at 420 nm (microflowers) or 450 (nanosheets) nm and a defect-related emission band extending from 500 to 650 nm. The UV emission is also called the near band edge emission (NBE) which is due to the exciton recombination [35]. The deep level emission (DLE) is in the range of 500–650 nm. It is also regarded as the green emission which is resulted from some defects, such as the vacancies of Zn in ZnSe [36, 37]. By calculating the data, the I_{UV}/I_{DLE} of ZnSe microflowers and nanosheets are 0.32 and 3.78, respectively. As we all know, the higher I_{UV}/I_{DLE} indicates the better crystalline property. Therefore, ZnSe nanosheets have higher crystalline quality than ZnSe microflowers. On the contrary, ZnSe microflowers have more defects than ZnSe nanosheets.

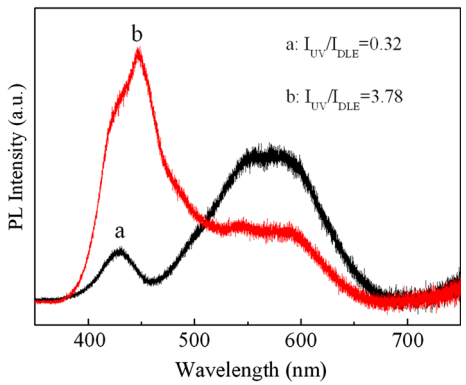

Fig. 5 Room-temperature photoluminescence of ZnSe microflowers (*a*) and nanosheets (*b*)

To evaluate the photocatalytic activity of the as-prepared ZnSe with different morphologies, the photocatalytic degradation experiment of RhB was carried out, and the curves of degradation efficiency versus irradiation time are shown in Fig. 6. The blank experiment of photocatalytic degradation of RhB in the absence of any catalysts reveals that the photoinduced self-sensitized photolysis of RhB can be neglected. In contrast, photocatalytic degradation was highly enhanced with the assistant of ZnSe samples, and the photocatalytic efficiency depends on their morphologies. After 8 h irradiation under ultraviolet light, the degradation efficiency of RhB reaches 94.3 and 82.3 % in the presence of ZnSe microflowers and nanosheets, respectively. Clearly, ZnSe microflowers exhibits superior photocatalysts compared to nanosheets.

It is generally accepted that the photocatalytic activity of micro/nanomaterials strongly depends on their sizes. The sample with smaller size exhibits higher photocatalytic activity than the sample with bigger size. However, ZnSe microflowers with big size show more excellent photocatalytic activity than that of nanosheets in our experiment. This is because the photocatalytic activity of ZnSe micro/nanomaterials is also influenced by the defects [7].

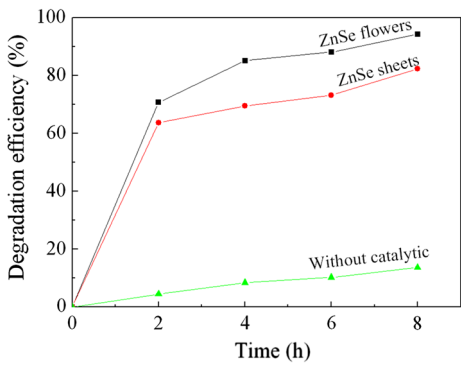

Fig. 6 Comparison of the photocatalytic activities of ZnSe micorflowers and nanosheets

When ZnSe photocatalysts are irradiated by UV light, photoelectrons and photoholes (electron–hole pairs) will be generated. At the same time, the chance of generation and recombination of electron–hole pairs is equal. As we all know, the photocatalytic activity of catalysts will reduce with the recombination of electron–hole pairs. The defects of ZnSe micro/nanomaterials are beneficial to the efficient separation of electron–hole pairs, and the recombination of electron–hole pairs can be effectively inhibited. Furthermore, the surface defects of ZnSe micro/nanomaterials can absorb oxygen species (such as O^{2-}, OH^{-}) that will change into high-activity OH^{-} and O^{2-} which should improve the catalytic reaction [7]. Figure 5 shows that the defect-related emission from ZnSe microflowers is relatively stronger than that of ZnSe nanosheets, indicating that more surface defects exist in the microflowers. So, the photocatalytic ability of ZnSe microflowers is stronger than that of nanosheets.

4 Conclusions

ZnSe microflowers and nanosheets were synthesized via a solvothermal process and subsequent annealing treatments. The thermal decomposition of the precursors $ZnSe(en)_{0.5}$ produced ZnSe, and the original morphology was preserved throughout the process. In addition, the photocatalytic activities of the ZnSe microflowers and nanosheets for the degradation of RhB under the irradiation of UV light were investigated. ZnSe microflowers exhibited superior photocatalytic activity in the photodegradation of RhB under UV light irradiation because ZnSe microflowers have more defects.

Acknowledgments This work is supported by the National Natural Science Foundation of China (Grant Nos. 61378085, 61308095, 51479220, 51441006 and 11254001), program for the development of Science and Technology of Jilin province (Item Nos. 20140101205 JC, 20130102004JC, 20150520086JH and 201215222), the twentieth five-year program for Science and Technology of Education Department of Jilin province (20140155).

References

1. Y. Zhong, J.F. Wang, R.F. Zhang, W.B. Wei, H.M. Wang, X.P. Lü, F. Bai, H.M. Wu, R. Haddad, H.Y. Fan, Nano Lett. **14**, 7175–7179 (2014)
2. K. Rajeshwar, A. Thomas, C. Janáky, J. Phys. Chem. Lett. **6**, 139–147 (2015)
3. F. Cao, W.D. Shi, L.J. Zhao, S.Y. Song, J.H. Yang, Y.Q. Lei, H.J. Zhang, J. Phys. Chem. C **112**, 17095–17101 (2008)
4. L.H. Zhang, H.Q. Yang, J. Yu, F.H. Shao, L. Li, F.H. Zhang, H. Zhao, J. Phys. Chem. C **113**, 5434–5443 (2009)
5. L.L. Chen, W.X. Zhang, C. Feng, Z.H. Yang, Y.M. Yang, Ind. Eng. Chem. Res. **51**, 4208–4214 (2012)
6. S.L. Xiong, B.J. Xi, C.M. Wang, G.C. Xi, X.Y. Liu, Y.T. Qian, Chem. Eur. J. **13**, 7926–7932 (2007)
7. B. Feng, J. Cao, J.H. Yang, S. Yang, D.L. Han, Mater. Res. Bull. **60**, 794–801 (2014)
8. J.L. Xu, W. Wang, X. Zhang, X.J. Chang, Z.N. Shi, G.M. Haarberg, J. Alloys Compd. **632**, 778–782 (2015)
9. Y. Zhang, C.G. Hu, B. Feng, X. Wang, B.Y. Wan, Appl. Surf. Sci. **257**, 10679–10685 (2011)
10. B. Feng, J.H. Yang, J. Cao, L.L. Yang, M. Gao, M.B. Wei, H.J. Zhai, Y.F. Sun, H. Song, J. Alloys Compd. **555**, 241–245 (2013)
11. A.L. Weaver, D.R. Gamelin, J. Am. Chem. Soc. **134**, 6819–6825 (2012)
12. S. Sarkar, S. Acharya, A. Chakraborty, N. Pradhan, J. Phys. Chem. Lett. **4**, 3292–3297 (2013)
13. F. Ashrafi, S. Mohammad, H. Feiz, H.R. Fallah, M.H. Yousefi, M.H. Shivaee, J. Mater. Sci. Mater. Electron. **25**, 1880–1886 (2014)
14. D.L. Han, B. Feng, J. Cao, M. Gao, S. Yang, J.H. Yang, J. Mater. Sci. Mater. Electron. **25**, 3639–3644 (2014)
15. K. Yadav, Y. Dwivedi, N. Jaggi, J. Mater. Sci. Mater. Electron. **26**, 2198–2204 (2015)
16. J.P. Zhuang, Y. Liang, X.D. Xiao, S.K. Hark, J. Phys. Chem. C **116**, 8819–8823 (2012)
17. G.Y. Feng, C. Yang, S.H. Zhou, Nano Lett. **13**, 272–275 (2013)
18. J.Q. Hu, Y.S. Bando, J.H. Zhan, Z.W. Liu, D. Golberg, S.P. Ringer, Adv. Mater. **17**, 975–979 (2005)
19. S. Arya, S. Khan, P. Lehana, I. Gupta, S. Kumar, J. Mater. Sci. Mater. Electron. **25**, 4150–4155 (2014)
20. B. Feng, J.H. Yang, J. Cao, L.L. Yang, M. Gao, M.B. Wei, H.J. Zhai, Y.F. Sun, H. Song, J. Alloys Compd. **555**, 241–245 (2013)
21. Z.X. Deng, C. Wang, X.M. Sun, Y.D. Li, Inorg. Chem. **41**, 869–973 (2002)
22. Y.H. Ni, L. Zhang, L.X. Zhang, W. Wei, Cryst. Res. Technol. **43**, 1030–1035 (2008)
23. Z.D. Hu, X.F. Duan, M. Gao, Q. Chen, L.M. Peng, J. Phys. Chem. C **111**, 2987–2991 (2007)
24. P. Chen, T.Y. Xiao, H.H. Li, J.J. Yang, Z. Wang, H.B. Yao, S.H. Yu, ACS Nano **6**, 712–719 (2012)
25. L. Jin, J. Wang, C.H. Wallace, Cryst. Growth Des. **8**, 3829–3833 (2008)
26. B. Goswami, S. Pal, C. Ghosh, P. Sarkar, J. Phys. Chem. C **113**, 6439–6443 (2009)
27. Y.Y. Yang, F.L. Du, C. Miao, Mater. Lett. **62**, 1333–1335 (2008)
28. W.D. Shi, J.Q. Shi, S. Yu, P. Liu, Appl. Catal. B Environ. **138–139**, 184–190 (2013)
29. L.H. Zhang, H.Q. Yang, L. Li, R.G. Zhang, R.N. Liu, J.H. Ma, X.L. Xie, F. Gao, Inorg. Chem. **47**, 11950–11957 (2008)
30. X.Y. Huang, H.R. Heulings, V. Le, J. Li, Chem. Mater. **13**, 3754–3759 (2001)
31. J. Lu, S. Wei, Y.Y. Peng, W.C. Yu, Y.T. Qian, J. Phys. Chem. B **107**, 3427–3430 (2003)
32. X. Ouyang, T.Y. Tsai, D.H. Chen, Q.J. Huang, W.H. Cheng, A. Clearfield, Chem. Commun. **6**, 886–887 (2003)
33. J.S. Jang, C.J. Yu, S.H. Choi, S.M. Ji, E.S. Kim, J.S. Lee, J. Catal. **254**, 144–155 (2008)
34. L. Volpe, M. Boudart, Catal. Rev. Sci. Eng. **275**, 15–538 (1985)
35. B.Y. Geng, Q.B. Du, X.W. Liu, J.Z. Ma, X.W. Wei, Appl. Phys. Lett. **890**, 33115 (2006)
36. Y.C. Zhu, Y. Bando, Chem. Phys. Lett. **377**, 367–370 (2003)
37. X. Wang, Y.D. Li, Angew. Chem. Int. Ed. **414**, 790–4793 (2002)